

# A spectrum-compatibility method for deriving earthquake-induced displacements of unstable slopes



**F. Bozzano, C. Esposito, S. Martino, A. Prestininzi & G. Scarascia Mugnozza**

*Department of Earth Sciences and Research Centre for Geological Risks (CERI), University of Rome (Italy) "La Sapienza"*

**G. Martini & D. Rinaldis**

*Italian National Agency for New Technologies, Energy and Sustainable Economic Development (ENEA), Rome (Italy)*

## SUMMARY

Ground-motion scenarios based on a spectrum-compatibility method were derived for evaluating the expected earthquake-induced displacements of unstable slopes in a test area (Southern Calabria - Italy). Natural time-histories were selected from the international catalogues with reference to seismological features of a specific seismic source (i.e. epicentral distance, magnitude, focal mechanism). A spectral attenuation was considered, according to the Sabetta and Pugliese Italian attenuation law, to define the expected response spectrum at the outcropping bedrock in correspondence to existing landslide areas, which resulted by a detailed local inventory-map. A compatibility between the spectrum of the selected natural time-histories and the local expected response spectrum was obtained; the corresponding time-histories were used to compute co-seismic displacements by the classic Newmark's method. Different scenarios of landslide re-activation were derived and the respective probability computed, by taking into account the local seismic sources as well as the geomechanical features attributed to each landslide mass.

*Keywords: Seismically-induced landslides, susceptibility analysis, Newmark's displacements, spectrum-compatible reference inputs, Southern Italy*

## 1. INTRODUCTION

Expected co-seismic displacements of slopes are commonly computed by applying Newmark's sliding block method (Newmark, 1965); according to this method, the landslide mass is assimilated to a rigid block on an inclined plane. The block has a critical acceleration  $k_y$  representing the threshold action required for sliding initiation. The Newmark's method makes it possible to calculate the cumulative co-seismic permanent displacement of a landslide mass forced by an acceleration time-history.

Based on the Newmark approach, some empirical equations were proposed by solving multivariate co-relations (Jibson et al., 1993; Jibson et al., 1998; Romeo, 2000; Hsieh & Lee, 2011) to provide the Newmark's displacement ( $D_N$ ) for known values of critical acceleration and ground-shaking parameters (i.e. PGA or Arias intensity). These co-relations represent useful tools for deriving expected  $D_N$  values within large areas by use of geographic information systems (GIS) and by performing a hazard-mapping procedure (Jibson et al., 2000). According to this procedure, both  $k_y$  and expected PGA are attributed to a spatial grid and  $D_N$  is automatically computed by applying the empirical co-relations. More in particular,  $k_y$  derives by combining information from a slope-gradient map (i.e., derived from a Digital Elevation Model) and from shear strength properties assigned to the outcropping lithologies; on the other hand, the expected PGAs derive from shaking maps, i.e. by attributing to each grid node a value of PGA expected for an earthquake scenario by applying a seismic attenuation law with respect to the epicentral distance.

The reliability of this approach was tested in California (Jibson et al., 1998; Jibson et al., 2000; Jibson, 2007) taking into account well documented seismically induced landslide effects due to the 17 January 1994 Northridge earthquake; maps of slope failures probability based on the Newmark's displacements were also proposed, referred to the shaking scenario of interest. The probabilistic

seismic landslide hazard-mapping procedure for Newmark's co-seismic slope displacements was applied so far by many Authors (Capolongo et al., 2002; Saygili & Rathje, 2009; Wang & Lin, 2010; Romeo et al., 2011; Vollmert et al., 2011); nevertheless, these applications are generally referred to slope failures, i.e. not specifically devoted to analyse co-seismic displacements due to re-activation of pre-existing landslide masses.

The interest of this topic lies in the complex interactions between seismic waves and pre-existing landslide masses which can cause significant differences in expected co-seismic displacements with respect to the Newmark's approach (Lenti & Martino, 2011).

At this aim, the here considered South-Tyrrhenian Calabria represents a significant test site since it is exposed to high magnitude earthquakes (related to Southern Italy seismogenetic source areas), as proved by the catastrophic earthquakes in 1783 ("Terremoto delle Calabrie" earthquake -  $M_w=6.5+$ ) and in 1908 ("Reggio and Messina" earthquake -  $M_w=7.0$ ).

To perform this study natural time-histories compatible with the expected response spectra were specifically derived for each landslide mass and for each considered earthquake scenario, as an alternative to a PGA shaking map; moreover, it was also taken into account the role of pore water pressures within the slopes by considering a variation of the  $r_u$  parameter along the landslide sliding surface.

## 2. GEOLOGICAL SETTING OF THE STUDY AREA

The study area corresponds to the South-Tyrrhenian portion of the Calabria region and it is part of the "Arco Calabro Peloritano" Mountain Chain; this sector can be considered a fore-arc/back-arc basin system and the corresponding geodynamic evolution is related to a complex combination of compressive and normal tectonic events due to the lithospheric subduction of the Ionian oceanic crust under the Calabrian Arc (Monaco et al., 1996); the Benioff plane has a NWward high angle dip below the Tyrrhenian sea up to more than 600 km of depth.

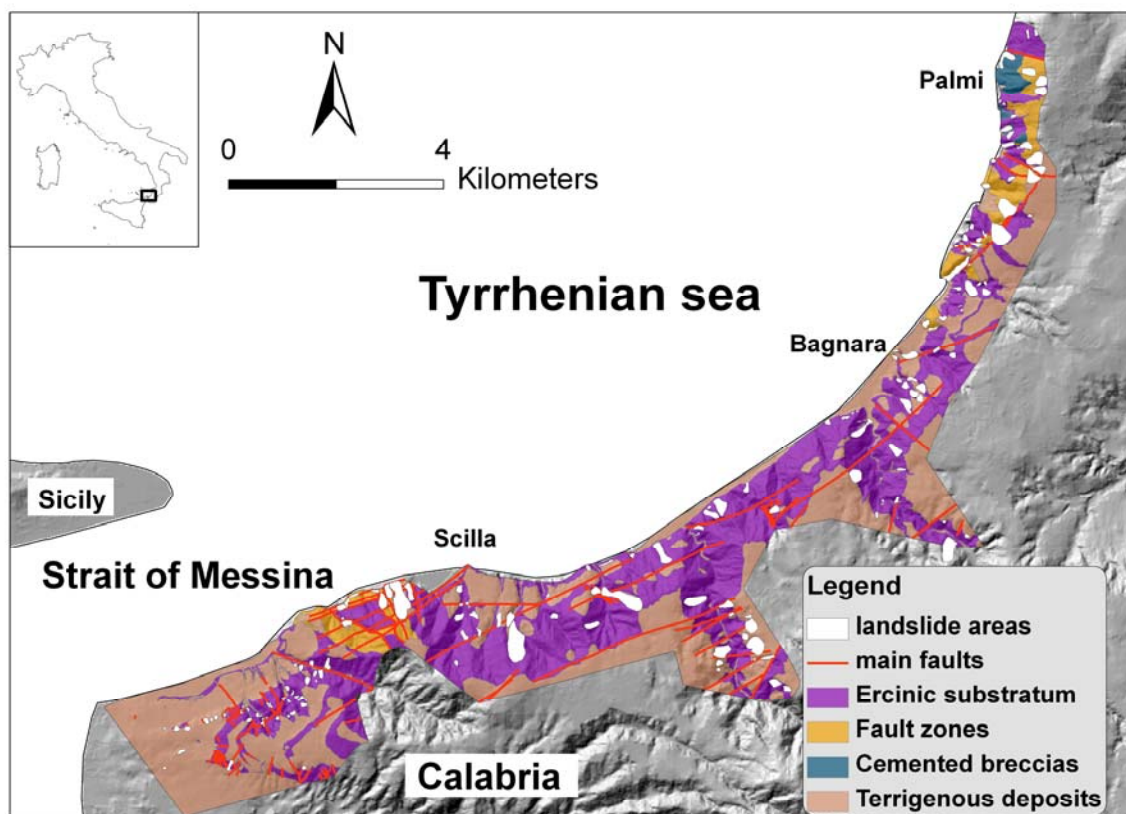


**Figure 1.** Geological map of the study area and location of the recognized landslides.

The stratigraphic succession outcropping in this area (Fig.1) is characterized by cemented rocks and granular deposits ascribable to the Ercinic-Holocene time interval. The Paleozoic basement is part of the Aspromonte metamorphic unit (Lentini et al., 2002; Carbone et al., 2008). These metamorphic rocks are characterised by a predominant isotropic, granular texture, including biotitic micas, plagioclastic minerals and rounded xenoliths. A major Alpine foliation is also detectable, and wide zones of cataclastic to mylonitic rocks generally correspond to the main fault lines. Also a thick succession of terrigenous transgressive deposits widely outcrop in the study area and it includes conglomerates, marls and sands, ascribable to the Tortonian-Pliocene time interval, passing to sands and gravel of the Pliocene-Holocene time interval and including marine terrace deposits. The intense tectonic evolution of this area is responsible for intense jointing of the rock masses which can be observed astride the main fault lines. Moreover, breccias of gneiss cemented by calcite, widely outcrop in the considered area.

### 3. LANDSLIDE INVENTORY

Several landslides affect the study area because of the morphological features of the relief (i.e. deepening rivers, cliff slopes) as well as of the geomechanical properties of the outcropping rock masses (i.e. highly jointed rock masses or poorly cemented granular deposits). 175 landslides were recognized so far, including 57 falls and 118 sliding, over an area of about 45 km<sup>2</sup>. More in particular, the sliding types include 94 roto-translational landslides and 24 translational landslides. The percentage Landsliding Index computed for the study area is almost equal to 6%. Moreover, about 80% of all the recognized landslides involves the metamorphic substratum, among which about 57% is represented by roto-translational landslides and 51% by falls (Fig.2).

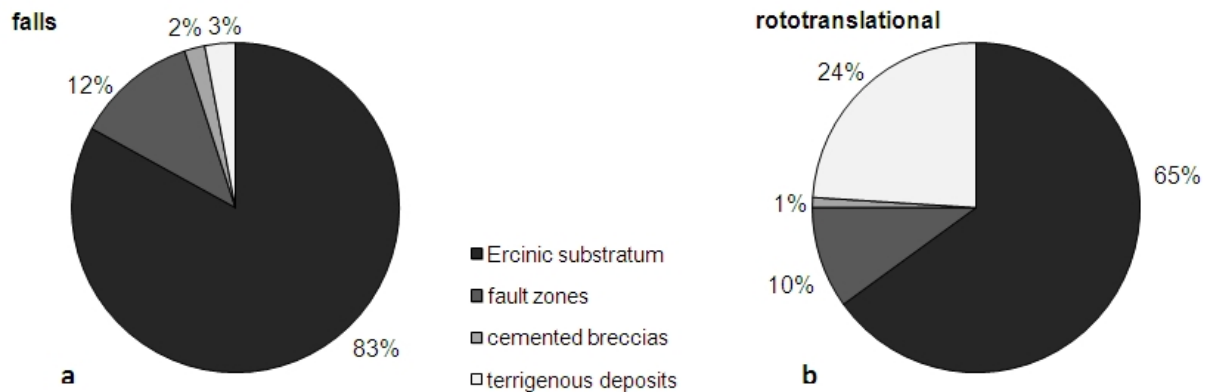


**Figure 2.** Percentages of fall (a) and of roto-translational (b) landslides involving different lithologies.

The largest event within the study area is represented by the Mt. Pacì rockslide triggered by the earthquake occurred on 6 February 1783, during the “Terremoto delle Calabrie” seismic sequence. This rockslide involved about 8Mm<sup>3</sup> and induced a tsunami wave responsible for more than 1500 casualties in the neighbouring Marina Grande beach (Gerardi et al, 2006; Graziani et al, 2006; Bozzano et al., 2011).

### 4. SUSCEPTIBILITY ANALYSIS OF LANDSLIDES

As a preliminary step, a simple landslide susceptibility analysis was performed in order to point out the relationships among the high occurrence of falls and roto-translational slope instabilities and the potential predisposing “environmental” factors. Use was made of the Frequency Ratio model, whose reliability has been proved for susceptibility assessment purposes (e.g.: Yilmaz 2009, Lee & Sambath 2006). This method is based on the use of frequency ratio (FR), the ratio of landslide occurrence

probability to a non-occurrence for a given attribute (Lee & Talib, 2005). The main advantage of this method relies on its complete implementation within a GIS environment. Ten different types of factors were used to calculate the frequency ratios: lithological units, land-cover units, distance from faults, morphometric (slope, aspect and curvature) and hydraulic (topographic wetness index) parameters derived from an available 20m resolution DEM. Subsequently the landslide susceptibility index ( $LSI = \sum FR$ ) was evaluated. A validation of the prediction results was performed by partitioning the total area into two separated subareas, the North side and South side, using the space partition criterion defined by Chung & Fabbri (2003). Each part was used to set up a specific susceptibility model and, at the same time, to test the model set for the other area. The best susceptibility models and the related maps were evaluated by the estimation of the Success Rate Curve for each model and the respective Area Under Curve (AUC) both for falls and slides.

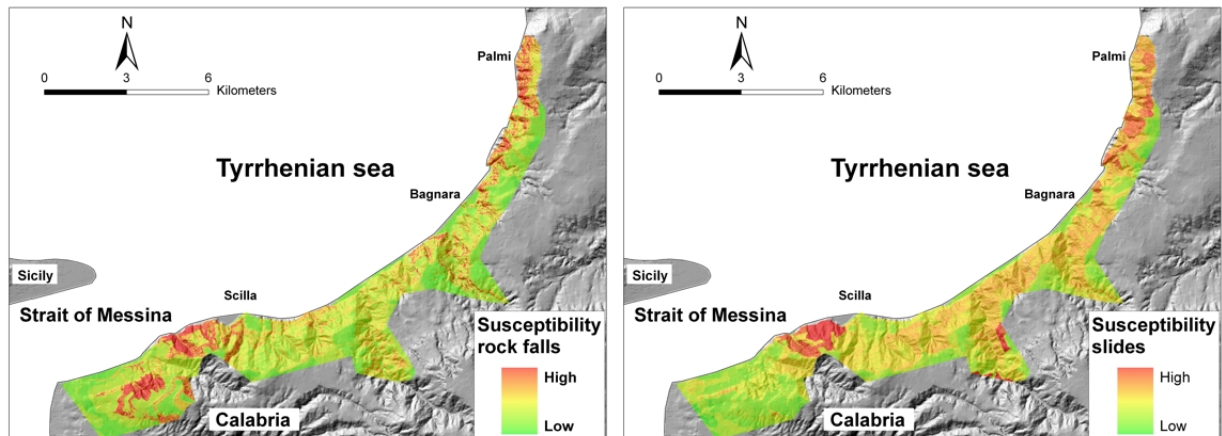


**Figure 3.** Susceptibility map of landslides obtained for the study area referred to falls (left) and to rotational landslides (b).

The so derived maps show that a high susceptibility to falls involves the coastline characterised by cliff slopes in the northern part of the study area as well as some river valley characterised by the wide outcropping of low cemented Plio-Pleistocene sands. As it results from the here performed susceptibility analysis, in addition to the dip of the slope also the outcropping breccias and the intensely jointed fault zones correspond to areas particularly prone to landslide events.

## 5. SCENARIOS OF SEISMICALLY-INDUCED LANDSLIDE RE-ACTIVATIONS

### 5.1. Derivation of spectrum-compatible accelerometric time histories

In order to derive scenarios of earthquake-induced landslide re-activation, 6 seismogenetic source areas were considered here, based on the INGV on-line Database of Individual Seismogenetic Sources (DISS); moreover, another source was hypothesized in this study, located in the Tyrrhenian sea off-shore and constrained by the numerous earthquakes recorded by the National Accelerometric Network. The 7 selected seismic sources are reported in the following Table 5.1

**Table 5.1.** Considered seismic sources.

Name	Reference earthquake	Mw
Aspromonte Northwest	6 February 1783	5.3
Scilla off-shore	16 November 1984	5.3
Aspromonte Northeast	16 November 1984	5.8
Subduction	not available	6.0
Gulf of Patti	15 April 1978	6.1
Gioia Tauro	5 February 1783	6.6
Strait of Messina	28 December 1908	7.0

To each seismogenetic source was attributed the uniform hazard spectrum (UHS), (Meletti & Montaldo, 2007; Montaldo & Meletti, 2007) corresponding to a recurrence time of 475 years, i.e. to a probability of exceedance of 10% in 50 years, except for the here hypothesized off-shore Tyrrhenian source to which a recurrence time of 2475 years, i.e. a probability of exceedance of 2% in 50 years, was attributed due to the lack of a reference earthquake. As the original UHS were calculated for the whole Italian territory on an 5 km equally spaced grid, a selection of UHS adjacent to each seismogenetic source was performed and a final UHS at the 90<sup>th</sup> percentile was calculated.

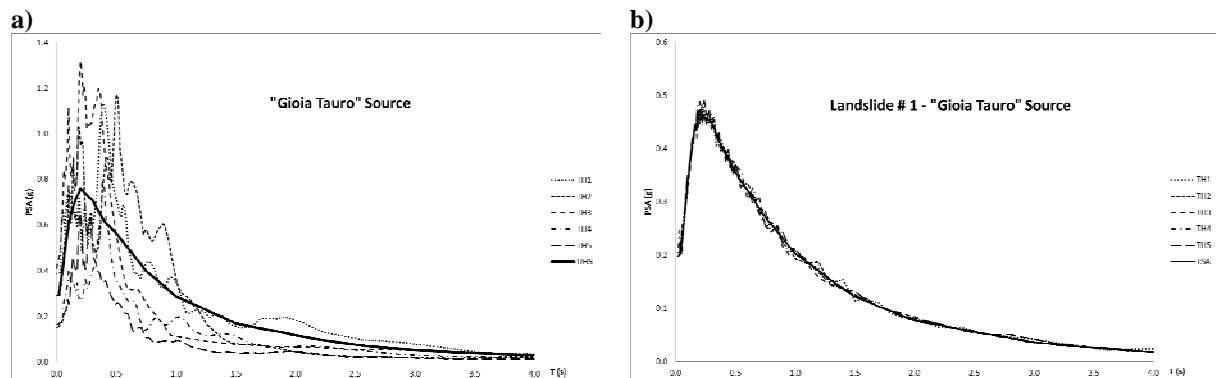


**Figure 4.** a) Example of UHS derived at the 90% percentile for “Gioia Tauro” seismogenetic source compared with the response spectra of the 5 natural time-histories selected from the global accelerometric catalogues; b) Example of compatible response spectra of the 5 time-histories selected for “Gioia Tauro” seismogenetic source, obtained by the spectrum-compatibility procedure applied to the response spectrum calculated by attenuation law for the landslide # 1.

In order to characterize the possible ground-motion generated by each seismogenetic source, a selection of natural accelerometric records was obtained by consulting both the European (Ambraseyes et al., 2000) and some global database of accelerometric records (COSMOS - <http://db.cosmos-eq.org>; PEER - <http://peer.berkeley.edu/smcat>; Kyoshin Network K-NET - <http://www-k-net.bosai.go.jp/k-net/index.en.shtml>). This selection was performed by considering the following criteria: i)  $M_w$  of the reference earthquake; ii) a circular area close to 30km from the epicentral zone, to better represent the near field ground-motion; iii) records obtained on outcropping seismic bedrock. The response spectra calculated for the set of time-histories selected for each seismogenetic source was compared with the relative 90<sup>th</sup> percentile UHS on the base of a shape criterion, as to obtain 5 natural accelerometric records that can be considered the expected ground-motion in the near-field area corresponding to the relative level of seismic hazard.

Moreover, in order to derive the possible accelerometric time-history at each recognized landslide, i.e. in correspondence with its centroid, the Sabetta & Pugliese (1996) attenuation law was used to calculate the local response spectra by measuring the epicentral distance of the landslide centroid and by using different empirical attenuation functions referred to 14 frequency values within 0.25 and 25 Hz. The 5 selected accelerometric records selected for each seismogenetic source were adapted to the response spectra calculated by attenuation law, on the basis of the procedure performed by the WES RASCAL CODE (Naeim & Lew, 1995) and modified with respect to the one previously proposed by Silva & Lee (1987). According to this procedure, the response spectrum of each time-history was modified by an original algorithm (Rinaldis et al., 2011) subtracting and/or adding contributions to the frequency content of the selected natural time-history.

Among the so derived 4130 time-histories (i.e. 5 for 7 seismogenetic sources and for 118 landslides) only 826 have been used for computing the co-seismic displacements by the Newmark method, i.e. the ones characterized by the highest Arias intensity computed for each landslide and for each seismogenetic source.

## 5.2. Scenarios of earthquake-induced landslide displacements

To evaluate the slope stability of the existing landslide masses under dynamic conditions a limit

equilibrium analysis was carried out for the roto-translational landslides only by applying the Bishop's method. In this regard two external actions were taken into account: the water pressure (related to the Bishop parameter  $r_u$ ) and the earthquakes, these latter considered as a pseudo-static forces applied at the barycentre of the landslide mass. These factors are closely related both with the seismicity of this area and with the occurrence of high intensity rainfall events that periodically affect the Calabria region.

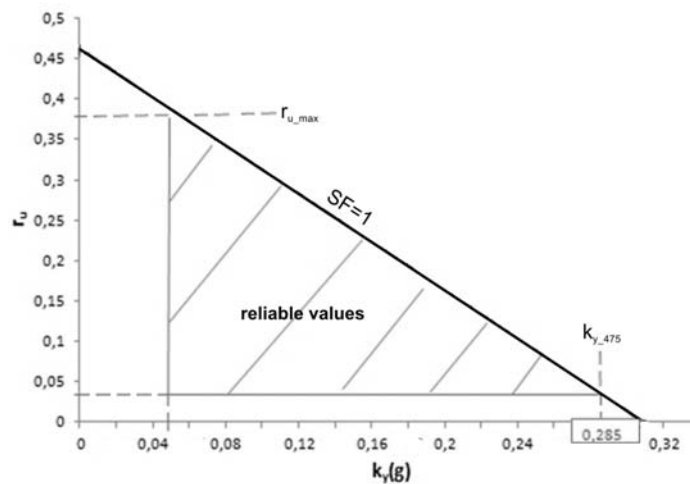


**Figure 5.** Example  $r_u$ - $k_y$  curve derived for one of the landslide masses recognized within the study area; limit values of  $r_u$  and  $k_y$  are also indicated.

In a first step, a sensitivity analysis was performed by evaluating the co-relation of the safety factor (SF) with each considered action. In a second step, the combination of the two parameters was considered leading to the construction for each landslide of a set of “critical”  $r_u$ - $k_y$  values, i.e. for SF=1.

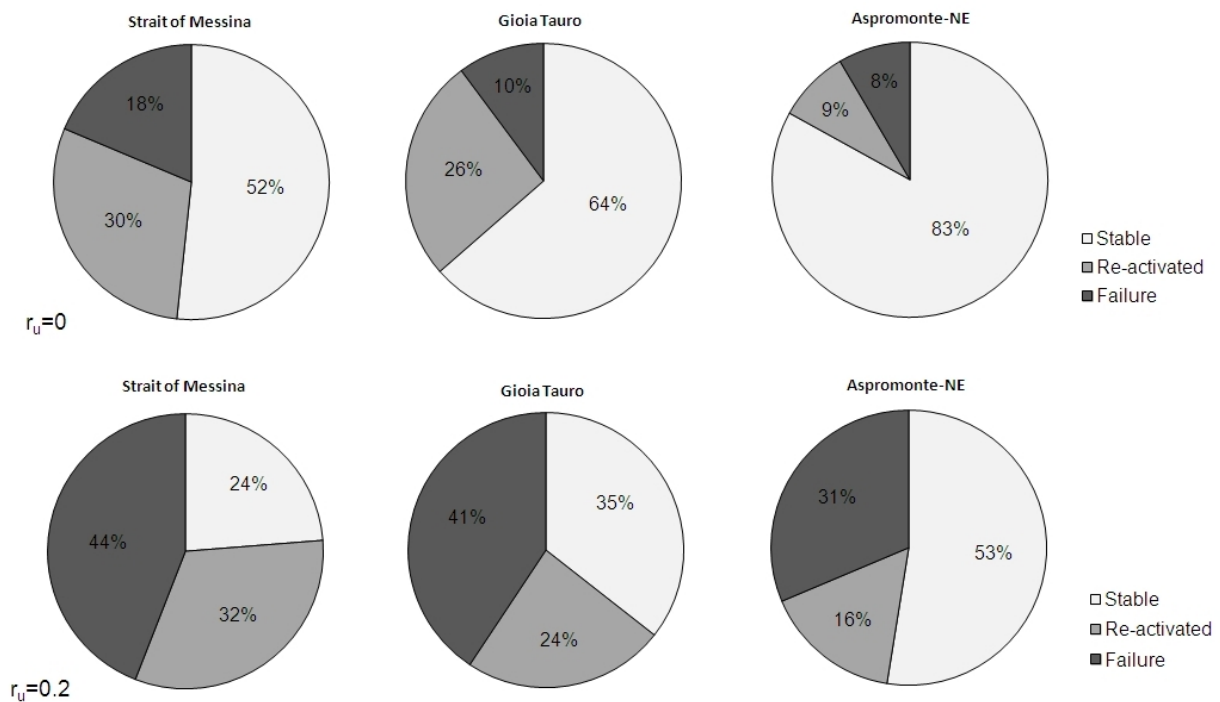


**Figure 6.** Percentages of earthquake re-activated landslide areas in case of different seismic sources (the Strait of Messina, Gioia Tauro and Aspromonte-NE) and for different  $r_u$  values.

Such critical values are constrained by two thresholds: the maximum  $r_u$ , fitting with the morphologic characteristics of the slopes, and the maximum critical acceleration, constituted respectively by the values of ground acceleration at probabilities of exceedance of 2% and 10% in 50 years for each landslide.

On this basis, a slope stability analysis for seismically-induced reactivation was performed through both isoprobabilistic and deterministic scenarios. In the first case, three different regression equations, developed in literature studies by Jibson et al. (1998), Romeo (2000) and Hsieh & Lee (2011), were used to correlate the Arias intensity of the seismic event, the critical acceleration and the co-seismic displacement. Displacement maps have been produced for return periods of 475 years and 2475 years. On the other hand, deterministic scenarios were obtained considering seven different sources, six of which extracted by the INGV-DISS catalogue and chosen in the Calabrian-Sicilian area with a  $M_w$  varying in the range 5.3-7.0. These UHS accelerometric time-histories derived by the previously described procedure (cfr. §5.1) were used to calculate the co-seismic displacement for all the roto-translational landslides by applying the sliding-block Newmark's method. The Newmark displacements were computed in relation to the different considered sources as well as to different values of  $r_u$ .

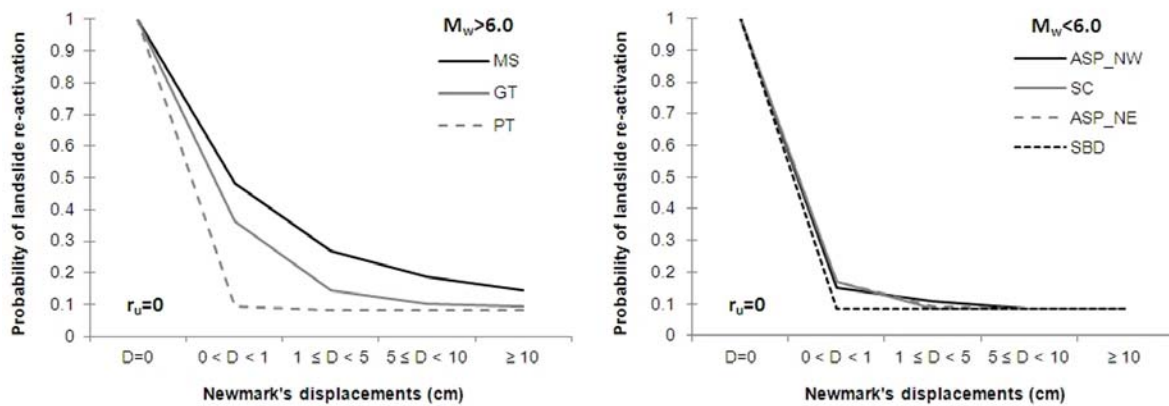


**Figure 7.** Probability of seismic landslide re-activation in the case of  $M_w > 6$  (left) and  $M_w < 6$  (right) earthquake scenarios for  $r_u = 0$ . Key to legend: MS – Strait of Messina; GT – Gioia Tauro; PT – Gulf of Patti; ASP\_NW – Aspromonte NW; SC – Scilla; ASP\_NE – Aspromonte NE; SBO – Subduction.

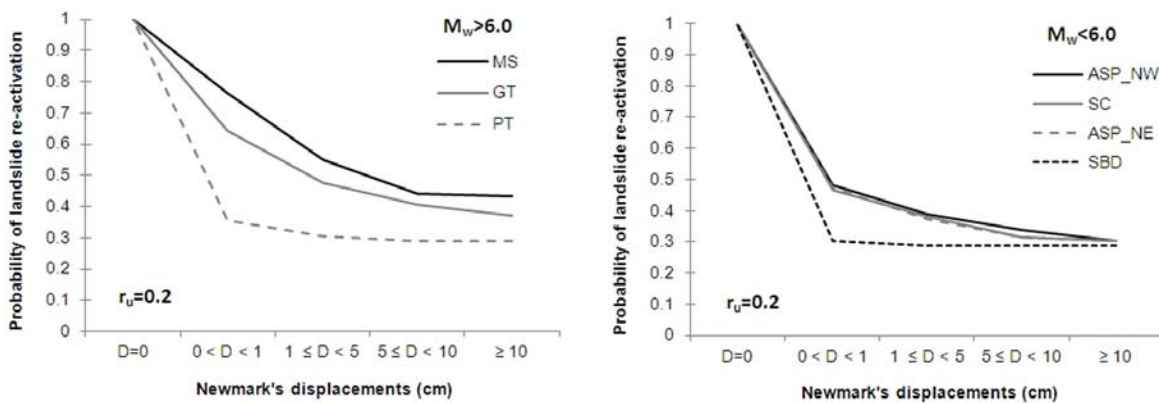


**Figure 8.** Probability of seismic landslide re-activation in the case of  $M_w > 6$  (left) and  $M_w < 6$  (right) earthquake scenarios for  $r_u = 0.2$ . Key to legend: MS – Strait of Messina; GT – Gioia Tauro; PT – Gulf of Patti; ASP\_NW – Aspromonte NW; SC – Scilla; ASP\_NE – Aspromonte NE; SBO – Subduction.

The so obtained co-seismic displacements were analysed in terms of “frequency distribution” to provide information on the percentage of the seismically re-activated landslides as well as on the extension of the involved area. These values were computed in relation to each considered seismic source and by considering different values of  $r_u$ . The reactivated landslides were distinguished from

failures in relation to the reached values of displacements according to Romeo (2000). As expected, the strongest scenario is represented by the Strait of Messina source for which the percentage of reactivated landslide area range from 33% up to 89%, considering  $r_u$  varying from 0 up to 0.4 (Fig.6). For the farthest sources individuated for this analysis the same parameter decrease down to 9% and to 50% for  $r_u=0$  and for  $r_u=0.4$  respectively, pointing out the importance of the distance between the seismic source and the landslide area.

Based on the frequency distribution of the earthquake re-activated landslides, a probability of re-activation was derived for each earthquake scenario and for different values of  $r_u$  (Figs 7,8).

As it results from this analysis, the highest earthquake scenario (i.e. the Strait of Messina one) implies a probability of 50% of producing not zero co-seismic displacements; more in particular, according to the values for co-seismic failures proposed by Romeo (2000), the probability of landslide collapses is equal to about 25%. This probability decreases to about 10% for the  $M_w=6.1$  Gulf of Patti earthquake scenario as well as for all the other  $M_w < 6$  earthquake scenarios. On the opposite, the probability of failure increases up to 50% for the Strait of Messina earthquake scenario by assuming a value of  $r_u=0.2$ .

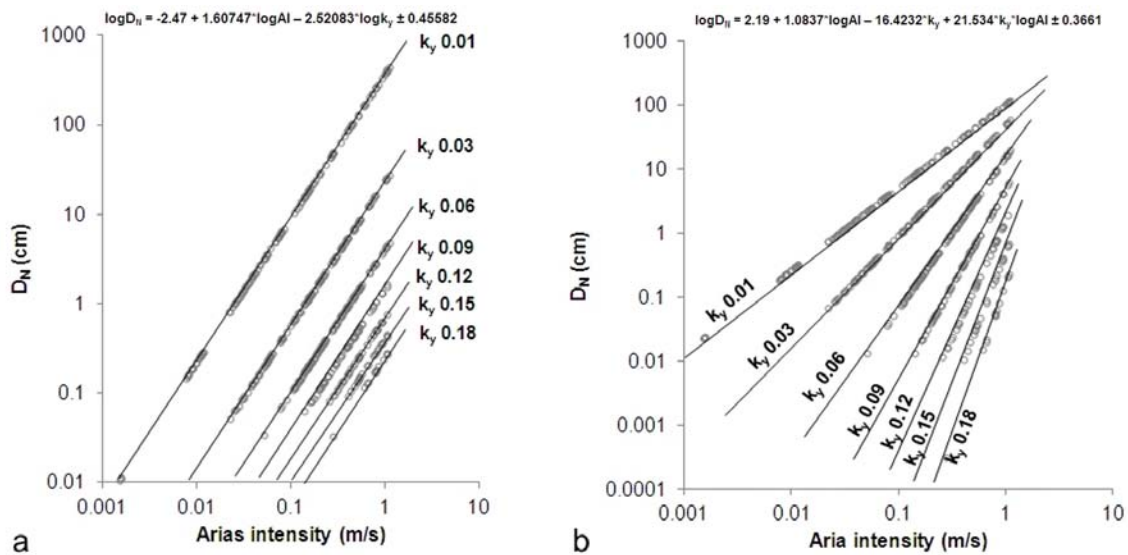


**Figure 9.** Empirical co-relations among Arias intensity,  $k_y$  and  $D_N$  obtained for the study area, according to the regression equations by Jibson et al. (1998) (a) and by Hsieh and Lee (2011) (b).

The spatial distribution of the re-activated landslides was also analyzed by dividing the total area in 8 equiangular azimuthal sectors to evaluate the percentage of seismically-induced landslide in each direction and to verify the distribution effects related to the seven sources. The obtained results show that the effects on the re-activation given by the highest magnitude scenario, i.e. the Strait of Messina source, are concentrated within  $135^\circ$ - $180^\circ$  azimuthal sectors. On the opposite, the scenarios whose  $M_w$  values range between 5.3 to 6.0 are characterized by a more uniform distribution of the effects in all the directions and by lower values of the percentages with respect to the strongest scenario described by the Strait of Messina source.

A validation of the regression models proposed by Jibson et al.(1998) and Hsieh & Lee (2011) was also performed by using the co-seismic displacement dataset, obtained for the studied landslides. A multivariate linear regression was carried out with the aim of producing specific regression equations for this area that can be used to estimate co-seismic displacement through the interaction between Arias intensity and the critical acceleration defined for each landslide. Good fit was achieved with respect to the literature data, in fact the relation obtained utilizing the Jibson (1998) model is characterized by a  $R^2$  of 0.79 while the relation by Hsieh and Lee (2011) model corresponds to a  $R^2$  of 0.86. It is worth stressing that such values were obtained using the complete datasets, thus avoiding subjective procedures for outliers detection and removal.

## 6. CONCLUSIONS

Based on the here discussed hazard-mapping procedure for earthquake induced landslides re-activation in the study area, the probability of slope collapses is about 25% for the highest expected earthquake scenario related to the Strait of Messina seismogenetic source. This probability significantly increases at increasing water pore pressures within the slope. Nevertheless it is worth noting that while in the case of earthquake scenarios it was possible to attribute a recurrence time to the event occurrence, on the opposite no sufficient constraints exist to evaluate the probability of occurrence of meteorological scenarios, i.e. related to intense rainfalls.

Moreover, since the here adopted Newmark's approach does not consider the physical interaction between seismic waves and pre-existing landslide masses the computed co-seismic displacements can be affected by systematic errors.

The here proposed procedure experienced the use of a UHS time-histories to force each landslide mass, instead of shaking maps of PGAs; these time-histories were derived according to a specific algorithm which adapt records selected from the accelerometric dataset to a local response spectrum referred to a specific probability of exceedance. Moreover a frequency-dependent attenuation law was applied to obtain the UHS time-histories at each landslide site.

## AKCNOWLEDGEMENTS

The Authors wish to thank S. Modanesi for her contribution to perform the slope stability analyses and for her assistance in the data processing. This research was funded by the project "POR-Calabria 2000-2006: Movimenti di massa ed attività sismotettonica" resp. Prof. G. Scarascia Mugnozza.

## REFERENCES

- Ambraseys, N., Smit, P., Berardi, R., Rinaldis, D., Cotton, F. and Berge-Thierry C. (2000). Dissemination of European Strong-Motion Data. CD-ROM collection. European Council, Environment and Climate Research Programme.
- Bozzano, F., Lenti, L., Martino, S., Montagna, A. and Paciello, A. (2011). Earthquake triggering of landslides in highly jointed rock masses: Reconstruction of the 1783 Scilla rock avalanche (Italy). *Geomorphology*, **129**, 294-308.
- Capolongo, D., Refice, A., and Mankelov, J. (2002). Evaluating earthquake-triggered landslide hazard at the basin scale through GIS in the upper Sele River valley. *Surveys in Geophysics*, **23**, 595–625.
- Carbone, S., Messina, A. and Lentini, F. (2008). Note Illustrative della carta geologica d'Italia alla scala 1:50.000: Foglio 601 . Dipartimento Difesa del Suolo, Servizio Geologico d'Italia. S.EL.CA. Firenze, 170pp.
- Chung, C. and Fabbri, F. (2003). Validation of spatial prediction models for landslide hazard mapping. *Natural Hazards*, **30**, 451-472.
- Gerardi, F., Barbano, M.S., De Martini, P.M. and Pantosti, D. (2006). Nature of tsunami sources (earthquake or landslide) in eastern Sicily and southern Calabria as inferred from historical data. 25° Convegno Nazionale GNGTS, Abstract, 63-66.
- Graziani, L., Maramai, A. and Tinti, S. (2006). A revision of the 1783 Calabrian (Southern Italy) tsunamis. *Natural Hazard and Earth System Sciences*, **6**, 1053-1060.
- Hsieh, S.Y. and Lee, C. T. (2011). Empirical estimation of the Newmark displacement from the Arias intensity and critical acceleration. *Engineering Geology*, **122**, 34-42.
- Jibson R.W., (2007). Regression models for estimating coseismic landslide displacement. *Engineering Geology* 91 (2007) 209–218
- Jibson, R.W., Harp, E.L. and Michael, J.M. (1998). A method for producing digital probabilistic seismic landslide hazard maps: an example from the Los Angeles, California Area. U.S. Geological Survey Open-File Report 98 – 113, 17pp.
- Jibson R.W., Harp L. and Michael J. A. (2000). A method for producing digital probabilistic seismic landslide hazard maps. *Engineering Geology*, **58**, 271-289.
- Jibson, R.W., (1993). Predicting earthquake-induced landslide displacement using Newmark's sliding block analysis. Transportation Research Board, National Research Council, Washington D.C., TR record 1411, 9–

- Lee, S. and Talib, J. A. (2005). Probabilistic landslide susceptibility and factor effect analysis. *Environmental Geology*, **47**, 982-990.
- Lee, S. & Sambath, T. (2006). Landslide susceptibility mapping in the Damrei Romel area, Cambodia using frequency ratio and logistic regression models. *Environmental Geology*, **50**, 847-856.
- Lenti, L. and Martino, S. (2011). The interaction of seismic waves with step-like slopes and its influence on landslide movements. *Engineering Geology*, 126 (2012) 19-36.
- Lentini, F., Catalano, S., Di Stefano, A. and Guarnieri, P. (2002). Stratigraphical and structural constraints in the Lucanian Apenins (Southern Italy): Tool for reconstructing the geological evolution. *Journal of Geodinamic*, **34**(1), 143-160.
- Meletti C., Montaldo V., 2007. Stime di pericolosità sismica per diverse probabilità di superamento in 50 anni: valori di ag. Progetto DPC-INGV S1, Deliverable D2, <http://esse1.mi.ingv.it/d2.html>
- Monaco, C., Tortorici, L., Nicolich, R., Cernobori, L. and Costa, M. (1996). From collisional to rifted basins: an example from the southern Calabrian arc (Italy). *Tectonophysics*, **266**, 233 – 249.
- Montaldo V., Meletti C., 2007. Valutazione del valore della ordinata spettrale a 1sec e ad altri periodi di interesse ingegneristico. Progetto DPC-INGV S1, Deliverable D3, <http://esse1.mi.ingv.it/d3.html>
- Naeim, F. and Lew, M. (1995). On the Use of Design Spectrum Compatible Time Histories. *Earthquake Spectra*, **11**(1), 111-127.
- Newmark, N. M. (1965). Effects of earthquakes on dams and embankments. *Geotechnique* 15, 139 – 159.
- Rinaldis D., Pugliese A., Martini G. and Zini A. (2011). Analisi della pericolosità sismica di base. In Scarascia Mugnozza G. (Ed.) “La pericolosità sismica del Lazio”. *Italian Journal of Engineering Geology and Environment – Book Series*, cap. 3, pp. 21-55 (da rivedere, aggiungere autori).
- Romeo, R.W. (2000). Seismically induced landslide displacements: a predictive model. *Engineering Geology*, **58** (3/4), 337-351
- Romeo, R.W., Mari, M., Pappafico, G., Tiberi, PP., Gori, U., Veneri, F., Tonelli, G. and Paletta, C., (2011). Hazard and risk scenarios of landslides triggered by earthquakes. Proc. of the 2nd World Landslide Forum, 3-7 October 2011, Rome (Italy).
- Sabetta, F. and Pugliese A. (1996). Estimation of response spectra and simulation of nonstationary earthquake ground motions. *Bull. Seismol. Soc. Am.*, **86**(2), 337-352.
- Saygili, G. and Rathje, E.M. (2009). Probabilistically based seismic landslide hazard maps: An application in Southern California. *Engineering Geology*, **109**, 183-194.
- Silva, W.J. and Lee, K. (1987). WES RASCAL Code for Synthesizing Earthquake Ground Motion. Miscellaneous Paper S-73-1, Report No. 24 in the Series “State-of-the-Art for Assessing Earthquake Hazard in the United States”, US Army Engineer Waterways Experiment Station.
- Vollmert, A., Reicherter, K., Silva, P.G. and Fernandez-Steeger, T.M. (2011). Landslide mapping to analyse earthquake environmental effects (EEE) in Carmona, Spain – relation to the 1504 event? 2nd INQUA-IGCP-567 International Workshop on Active Tectonics, Earthquake Geology, Archaeology and Engineering, Corinth, Greece (2011).
- Wang, K.L. and Lin, M.L. (2010). Development of shallow seismic landslide potential map based on Newmark’s displacement: the case study of Chi-Chi earthquake, Taiwan. *Environmental Earth Sciences*, **60**, 775-785.
- Yilmaz, I. (2009). Landslide susceptibility mapping using frequency ratio, logistic regression, artificial neural networks and their comparison: A case study from Kat landslides (Tokat—Turkey). *Computer Geosciences*, **35**, 1125-1138.